



Research article

Sterigmatocystin induces autophagic and apoptotic cell death of liver cancer cells via downregulation of XIAP

Xu Chen^{a,b,1}, Zhengping Che^{b,1}, Jiajia Wu^b, Cheng Zeng^b, Xiao-long Yang^{c,**},
Lin Zhang^{a,***}, Zhenghong Lin^{a,b,*}

^a Chongqing University Jiangjin Hospital, Chongqing, 402260, PR China

^b School of Life Sciences, Chongqing University, Chongqing, 401331, PR China

^c The School of Pharmaceutical Sciences, South-Central Minzu University, Wuhan, 430074, PR China

ARTICLE INFO

Keywords:

Apoptosis

Autophagy

Liver cancer

Sterigmatocystin

XIAP

ABSTRACT

XIAP, or the X-linked Inhibitor of Apoptosis Protein, is the most extensively studied member within the IAP gene family. It possesses the capability to impede apoptosis through direct inhibition of caspase activity. Various kinds of cancers overexpress XIAP to enable cancer cells to avoid apoptosis. Consequently, the inhibition of XIAP holds significant clinical implications for the development of anti-tumor medications and the treatment of cancer. In this study, sterigmatocystin, a natural compound obtained from the *genus aspergillus*, was demonstrated to be able to induce apoptotic and autophagic cell death in liver cancer cells. Mechanistically, sterigmatocystin induces apoptosis by downregulation of XIAP expression. Additionally, sterigmatocystin treatment induces cell cycle arrest, blocks cell proliferation, and slows down colony formation in liver cancer cells. Importantly, sterigmatocystin exhibits a remarkable therapeutic effect in a nude mice model. Our findings revealed a novel mechanism through which sterigmatocystin induces apoptotic and autophagic cell death of liver cancer cells by suppressing XIAP expression, this offers a promising therapeutic approach for treating liver cancer patients.

1. Introduction

Liver cancer is one of the most common prevalent malignant tumors with poor prognosis. It is notorious due to the difficulty of early detection and lack of effective treatment [1,2]. Currently, the primary treatment for liver cancer is surgical intervention, with chemotherapy as adjuvant therapeutic method. However, chemical therapy can lead to serious side effects, such as nausea, vomiting, gastrointestinal symptoms, liver and kidney failure, and toxic damage [3], thus reducing the life quality of the patients. Hence, it is crucial to elucidate the fundamental mechanism of liver cancer pathogenesis and discover efficacious pharmaceutical interventions for its management.

Apoptosis is a crucial process in the regulation of cell growth and tissue homeostasis. There are two main pathways through which apoptosis can be initiated: extrinsic and intrinsic, both of which converge at the mitochondria [4,5]. These pathways are regulated by

* Corresponding author. Chongqing University Jiangjin Hospital, Chongqing, 402260, PR China.

** Corresponding author.

*** Corresponding author.

E-mail addresses: yxl19830915@163.com (X.-l. Yang), brucezhanglin@cqu.edu.cn (L. Zhang), zhenghonglin@cqu.edu.cn (Z. Lin).

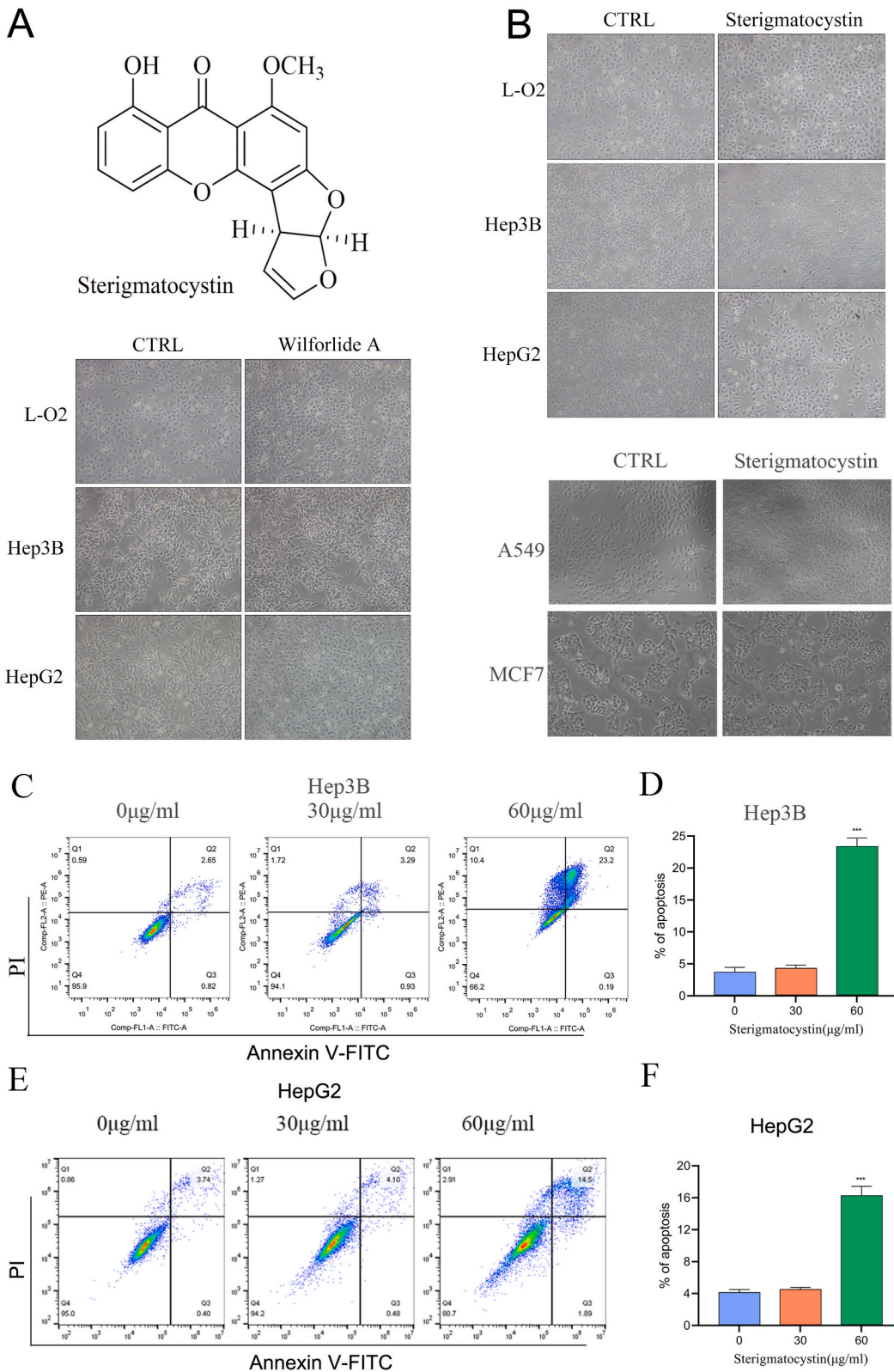
¹ Authors contributed equally to this work.

<https://doi.org/10.1016/j.heliyon.2024.e29567>

Received 5 November 2023; Received in revised form 9 April 2024; Accepted 10 April 2024

Available online 16 April 2024

2405-8440/© 2024 The Author(s). Published by Elsevier Ltd. This is an open access article under the CC BY-NC license (<http://creativecommons.org/licenses/by-nc/4.0/>).



(caption on next page)

Fig. 1. Sterigmatocystin induces the apoptosis of liver cancer cells. (A) The chemical structure of sterigmatocystin. (B) Various kinds of cell lines were treated with sterigmatocystin or Wilforlide A at a concentration of 60 $\mu\text{g/ml}$ for 24 h. (C) Apoptosis analysis of Hep3B cells treated with sterigmatocystin at concentrations of 0 $\mu\text{g/ml}$, 30 $\mu\text{g/ml}$, and 60 $\mu\text{g/ml}$ for 24 h, using flow cytometry after Annexin V-FITC and PI staining. (D) The percentage of apoptotic Hep3B cells treated with sterigmatocystin as indicated was shown. (E) The apoptosis of HepG2 cells was analyzed as in (C). (F) The percentage of apoptotic HepG2 cells was shown as in (D).

specific caspases, with initiator caspases (caspase-2, -8, -9, and -10) and effector caspases (caspase-3, -7, and -6) [6–8] playing key roles in the signaling cascade, which can be cleaved from their inactive zymogens [6,9,10]. Caspases, important enzymes in apoptosis, are regulated in living cells by inhibitors of apoptosis (IAP) proteins [11,12]. In human IAPs family, XIAP stands out as the sole member capable of directly blocking caspases and suppressing apoptosis [13], featured with three BIR domains that can bind directly to and inhibit caspase-9 along with a linker region responsible for inhibiting caspase-3 and -7 [14–16]. In addition, XIAP possesses a ubiquitin-associated (UBA) domain, which can bind to poly-ubiquitin chains, as well as a RING domain with E3 ubiquitin ligase activity [17–20]. Although the original study showed that XIAP deficient mice do not display any apparent phenotype, subsequent research reported that lymphoblastic leukemia and lymphomas can be developed in XIAP/ Δ RING mutant mice [18,21]. Moreover, inactivation of XIAP can enhance the susceptibility of specific stem cells to apoptosis [22,23] and its deletion or the absence of its RING domain can lead to excessive cell death [24]. XIAP is overexpressed in various kinds of cancers including thyroid carcinomas, colon, bladder, melanoma, ovarian, lung, prostate, renal, breast, and leukemia [25–27]. These cancers can overexpress XIAP, thus enabling tumor cells to escape apoptosis [28]. Therefore, targeting XIAP has become increasingly attractive for the treatment of cancers [28–31]. Except for its important role in the inhibition of apoptosis, XIAP has exhibited regulatory functions for autophagy in cells. It has been shown to inhibit autophagy and facilitate tumor progression by controlling the Mdm2-p53 pathway [32]. Clinical studies from Wu et al. showed that a negative association between XIAP levels and the autophagy biomarker LC3 in liver cancer samples [33]. These studies suggested that XIAP is involved in autophagy regulation.

Sterigmatocystin is a kind of metabolite extracted from fungi, which is an inhibitor of DNA synthesis and plays an inhibitory role in cell growth [34,35]. Previous studies have shown that sterigmatocystin can induce the release of cytochrome *c* and promote apoptosis of osteosarcoma cell lines U2OS and MG63 [36]. It can induce the activation of p21, inhibit the activity of CyclinD1/CDK4/6 complex, and block the proliferation of nasopharyngeal carcinoma cells [37]. In addition, although studies demonstrated its potential for the treatment of cancers, they are limited to osteosarcoma and nasopharyngeal carcinoma [36,37]. Up to date, there is no evidence of whether sterigmatocystin plays a role in the proliferation/apoptosis of hepatoma cells.

Our study revealed that sterigmatocystin can induce apoptosis in liver cancer cells. Utilizing RNA-seq, we conducted a transcriptome analysis of HepG2 cells treated with sterigmatocystin and identified differentially expressed genes through bioinformatics analysis. Our findings indicated a down-regulation of the XIAP gene whereas an up-regulation of apoptotic genes and autophagy-related genes in HepG2 cells treated with sterigmatocystin. Ultimately, these findings provide new insights into the underlying molecular mechanism of sterigmatocystin and its potential as a treatment for liver cancer.

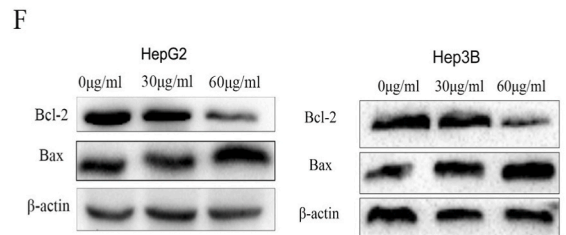
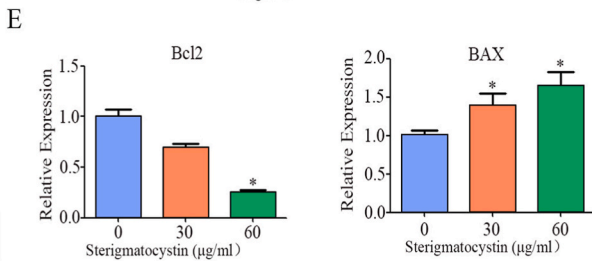
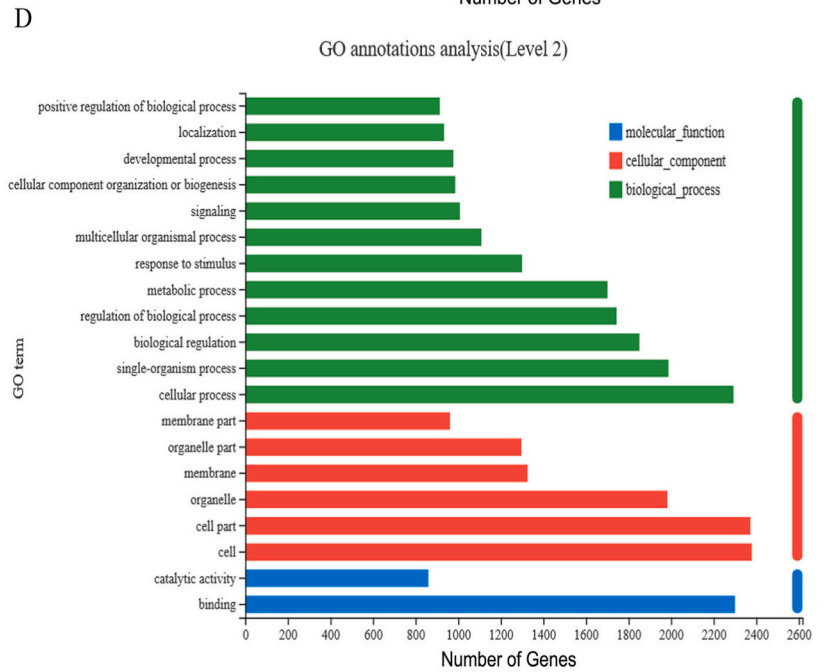
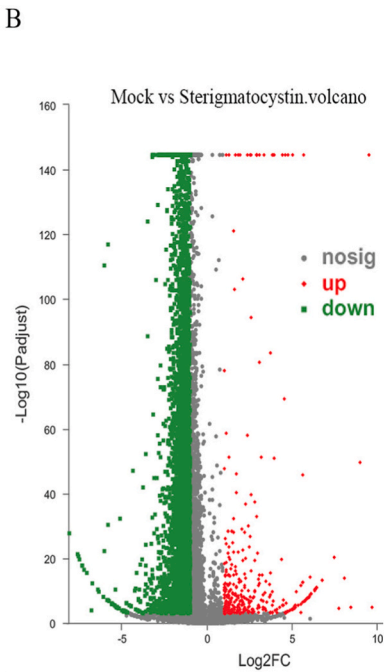
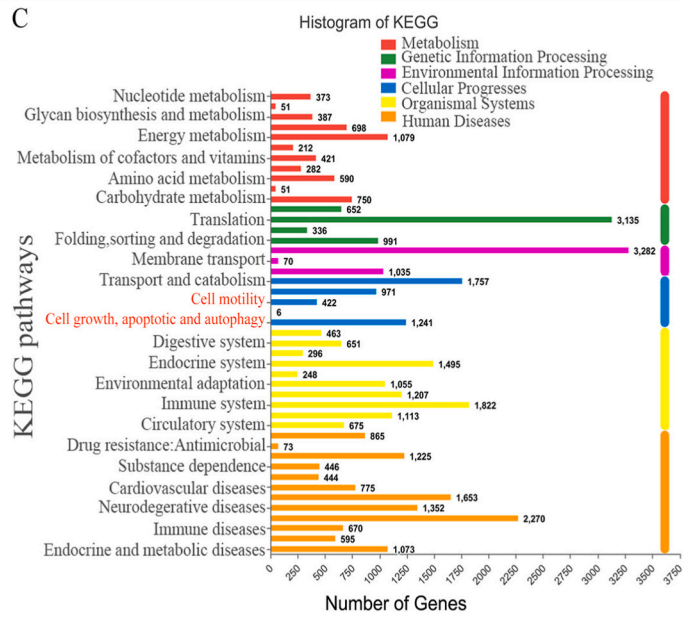
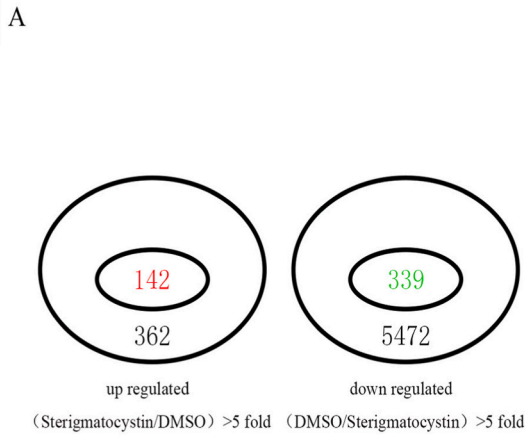
2. Materials and methods

2.1. Cell culture and reagents

Human normal hepatocyte cell line (L-O2) and Human liver cancer cell lines (HepG2, Hep3B) were purchased from the Procell Life Technology Company (Wuhan, China); Human lung cancer cell line (A549) and human breast cancer cell line (MCF7) were obtained from the Cell Bank of Chinese Academy of Sciences (Shanghai, China). They were cultured in DMEM supplemented with 10 % fetal bovine serum (FBS) and 100 U/ml mixture of penicillin and streptomycin, and were incubated at 37 °C and 5 % CO₂. Sterigmatocystin was dissolved in methanol to prepare a 100 mM stock solution. Primary antibodies for western blotting against caspase3, cleaved-caspase3, PARP, cleaved-PARP, XIAP, and MIIP (diluted to 1:1000) were purchased from Zen Bioscience (Chengdu, China); Bcl2 and BAX antibodies (diluted to 1:1000) were purchased from Sangon company (Shanghai, China). β -actin and cyclinB1 antibodies (diluted to 1:1000) were purchased from Sigma company. BCAS3 antibody (diluted to 1:1000) was purchased from Bioworld (Beijing, China). Cell counting kit 8 was purchased from MCE. The Annexin V-FITC/PI Apoptosis Detection kit was obtained from CWBIO (Beijing, China).

2.1.1. Cell viability and colony formation assay

Cell viability was evaluated using the cell counting kit 8 (CCK8) method. Briefly, cells were plated in 96-well plates at a density of 5×10^3 each well and left to incubate overnight, subsequently, they were treated with various concentrations of sterigmatocystin and cultured for different time intervals of 0, 24, 48, 72, and 96 h, respectively. Following this, CCK8 reagent was added and incubated at 37 °C for 2 h, after which the absorbance was recorded at a wavelength of 450 nm. To conduct the clonogenic assay, 1×10^3 cells were plated in 60 mm cell culture dishes, and cells were pretreated with different concentrations of sterigmatocystin for 6 h, then, replaced sterigmatocystin contained medium with fresh medium to form colonies in 2–3 weeks. After the colonies had formed, they were treated with glutaraldehyde (6.0 % v/v) for fixation and stained with crystal violet (0.5 % w/v).



(caption on next page)

Fig. 2. Transcriptome analysis of sterigmatocystin-treated liver cancer cells. (A) Statistics of the number of up-regulated and down-regulated differentially expressed genes in the transcriptome. (B) Volcano plot showing differentially expressed genes upon sterigmatocystin treatment. (C) KEGG analysis of the signaling pathways of differentially expressed genes in the transcriptome. (D) GO term analysis of the signaling pathways of differentially expressed genes in the transcriptome. (E) The mRNA level of Bcl2 and BAX were determined by real-time quantitative PCR after treatment with sterigmatocystin at concentrations of 0 $\mu\text{g/ml}$, 30 $\mu\text{g/ml}$, and 60 $\mu\text{g/ml}$ for 24 h. (F) The protein expression levels of BAX and Bcl2 were examined by western blot in HepG2 or Hep3B after treatment with sterigmatocystin at concentrations of 0 $\mu\text{g/ml}$, 30 $\mu\text{g/ml}$, and 60 $\mu\text{g/ml}$ for 24 h. β -actin was used as loading control.

2.2. Flow cytometric analysis

Hep3B and HepG2 cells were plated in 6-well plate and attached overnight. The cells were then treated with sterigmatocystin for 24 h. Subsequently, cells were collected and stained using Annexin V-FITC/PI apoptosis detection kit following the manufacturer's protocol. To analyze the cell cycle, the cells were incubated with indicated concentration of sterigmatocystin for 24 h, washed with pre-cooled PBS and fixed in 75 % alcohol overnight at 4 °C. The cells were then digested with 1 % RNase A and stained with 1 mg/ml PI for 30 min. All procedures were conducted according to the manufacturer's instructions, and the experimental data were analyzed using Flow Jo and Modifit software.

2.2.1. Quantitative real-time PCR

HepG2 cells were used for total RNA extraction using Trizol reagent (Invitrogen, Carlsbad, CA, USA). Removal of genomic DNA contamination was carried out by treating 10 μg of total RNA with DNase I (TaKaRa Bio Inc., Kusatsu, Japan). Following this, the resulting 1 μg total RNA was used in reverse transcription with M-MLV reverse transcriptase (TaKaRa). The quantitative real-time PCR analysis was performed on the ABI7500 instrument with gene-specific primers using SYBR premix ExTaq (TaKaRa). The following qRT-PCR primers were used: Bcl2, forward: CTCGTCGCTACCGTCGTGACTTCG, reverse: CAGATGCCGGTTCAGGTACTCAGTC, BAX, forward: AAGCTGAGCGAGTGTCTCCGGCG, reverse: GCCACAAAGATGGTCACTGTCTGCC, Caspase3, forward: AGAGAA-CAATGGCGGATA, reverse: CCAGTTGAGGGATGAAAG, XIAP, forward: ACCGTGCGGTGCTTTAGTT, reverse: TGC GTGGCAC-TATTTTCAAGATA, GAPDH, forward: TGA CTTCAACAGCGACACCCA, reverse: CACCCTGTTGCTGTAGCCAAA. Relative levels of interesting genes were normalized to β -actin by using the $2^{-\Delta\Delta\text{CT}}$ method.

2.3. Western blotting analysis

Cells were washed in pre-cooled PBS and total proteins were extracted using RIPA lysis buffer supplemented with protease inhibitors. The extracted proteins were then separated using sodium dodecyl sulfate-polyacrylamide gel electrophoresis (SDS-PAGE), transferred onto PVDF membranes, and immunoblotted with the corresponding primary antibodies overnight at 4 °C. Subsequently, the PVDF membranes were washed and incubated with secondary antibodies (1:5000) for 1 h at room temperature, and the immunoreactions were then visualized with chemiluminescent ECL reagent.

2.4. Wound healing assay

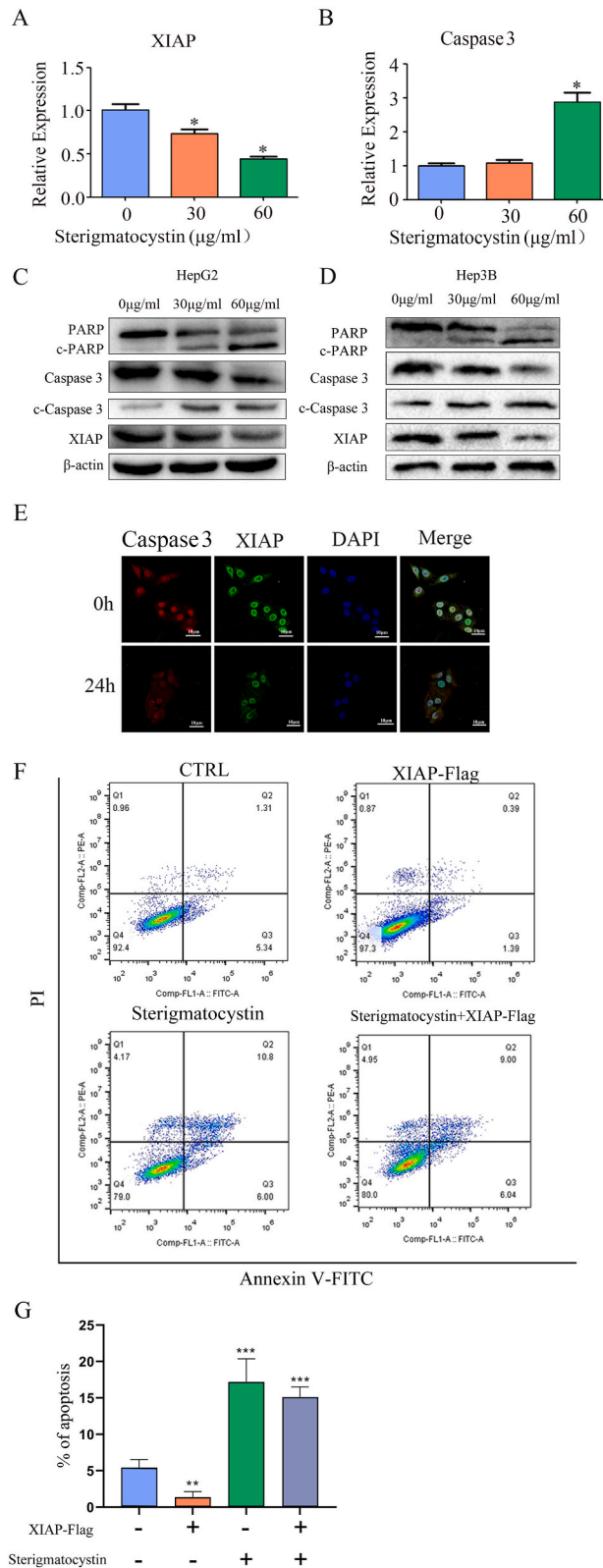
Cells were plated in a 60 mm cell culture dish and attached overnight. The next day, we use the tips to make a straightedge scratch. Cells were washed 3 times with PBS solution to remove free cells, and the cell culture medium was replaced with serum-free medium containing various concentrations of sterigmatocystin. Cells were put into a 37 °C 5 % CO₂ incubator and cultivated. Taking pictures at 0 and 12 h as indicated in the figures.

2.4.1. Transwell migration assay

Transwell assay was conducted following previously established protocols [38]. Briefly, cells were starved for 12 h before cell suspension preparation. The cell suspension was washed twice with PBS solution and resuspended in serum-free medium supplemented with BSA. The cell density was adjusted to $1 \times 10^5/\text{ml}$, and the cells were then inoculated and 100–200 μl of the cell suspension was added to the transwell chamber. Lift the chamber to remove air bubbles, then put the chamber into the culture plate. Culture cells for 24–48 h (mainly depending on the invasion ability of cancer cells). After the cells are stained, the cells can be counted under the microscope. Remove the Matrigel and cells in the upper chamber with a cotton swab, and stain with 0.1 % crystal violet. Use an upright microscope to observe and take pictures. By turning the transwell chamber upside down, the cells attached to the basement membrane of the chamber can be clearly observed.

2.4.2. Animal study

Approval was granted for all animal research by the Institutional Animal Care and Use Committee at Chongqing University (Protocol No: 2020L0018). In sum, 5×10^6 HepG2 cells were suspended in 100 μl of PBS and then injected subcutaneously into the flank of 6-week-old male nude mice. When the tumor volume reached $\sim 50 \text{ mm}^3$, the mice were randomly divided into different groups. Subsequently, sterigmatocystin (20 mg/kg) or PBS was injected intraperitoneally into the mice every two days. Tumor volume was recorded every five days. The mice were sacrificed after 20 days of treatment, and tumors were collected for analysis.



(caption on next page)

Fig. 3. Sterigmatocystin treatment downregulates XIAP expression. (A&B) The mRNA level of XIAP and Caspase3 in HepG2 cells was determined by real-time quantitative PCR after treatment with sterigmatocystin at concentrations of 0 $\mu\text{g/ml}$, 30 $\mu\text{g/ml}$, and 60 $\mu\text{g/ml}$ for 24 h. The error represents the SEM of three experiments. * $P < 0.05$. (C&D) The protein expression levels of PARP, cleaved PARP (c-PARP), Caspase 3, cleaved Caspase 3 (c-Caspase3), and XIAP were detected by western blot in HepG2 (C) or Hep3B (D) after treatment with sterigmatocystin at concentrations of 0 $\mu\text{g/ml}$, 30 $\mu\text{g/ml}$, and 60 $\mu\text{g/ml}$ for 24 h. β -actin was used as loading control. (E) The colocalization of XIAP and Caspase 3 was determined by microscope. HepG2 cells were treated with sterigmatocystin for 24 h or untreated (Scale bar, 10 μm). (F) Apoptosis analysis of Hep G2 cells treated with sterigmatocystin at concentrations of 60 $\mu\text{g/ml}$ for 24 h, using flow cytometry after Annexin V-FITC and PI staining.(G) The percentage of apoptotic HepG2 cells treated with overexpression of XIAP and sterigmatocystin alone and in combination as indicated was shown.

2.5. Statistical analysis

The comparison of mean values between 2 groups was conducted using the Student's t-test and one-way ANOVA. To determine the significance of repeated measurements over time and dosage, a two-way ANOVA was performed. In vivo experiments involving different groups were compared using a linear mixed-effects model that accounted for correlations within subjects. Multiple comparisons were assessed using Tukey's post hoc test. A value of $p < 0.05$ was considered statistically significant.

3. Results

3.1. Sterigmatocystin induces apoptosis of liver cancer cells

To investigate whether sterigmatocystin (Fig. 1A) has any effect in killing cancer cells, different types of cancer cells in the logarithmic growth phase were seeded on 96-well plates and treated with sterigmatocystin for 24 h. As shown in Fig. 1B, Hep3B and HepG2 cells showed remarkable apoptosis compared with normal hepatocytes while A549 and MCF7 cells exhibited no or less death. Also, another drug Wilforlide A had no impact on apoptosis in normal hepatocytes and hepatoma cells. Consistent with the above results, flow cytometric analysis of Hep3B and HepG2 cells treated with sterigmatocystin by Annexin V and PI staining showed a significant increase in apoptosis compared with untreated cells (Fig. 1C–F). Together, these data suggested that sterigmatocystin has a considerable anti-tumor effect by inducing apoptosis in liver cancer cells.

Transcriptome analysis identified the apoptotic- and autophagy-related genes as contributors to the sterigmatocystin-induced cell death.

To investigate the potential mechanism of apoptotic induction upon sterigmatocystin treatment, mRNA from drug-treated or untreated HepG2 cells was extracted and subjected to RNA sequencing. Among the differentially expressed genes (DEGs) in response to treatment with 60 $\mu\text{g/ml}$ sterigmatocystin, 142 genes were up-regulated (>5 fold) and 339 genes were down-regulated (>5 fold) (Fig. 2A&B). Further functional pathway analysis showed that these DEGs were involved in 23 pathways, including cell motility and cell growth, apoptotic and autophagy signaling, indicating that they were involved in the regulation of cell viability, apoptosis, and autophagy (Fig. 2C). GO database analysis indicated that the DEGs were mostly enriched in the cellular processes, and the molecular function (MF) terms "binding" (Fig. 2D). Subsequently, qRT-PCR was performed to study the changes in expression of genes related to apoptosis. As shown in Fig. 2E, Bcl2 gene showed a remarkable decrease of transcription in drug treated cells while BAX exhibited a dramatic increase. In accordance with above, western blot analysis showed a significant decrease in Bcl2 expression, while the expression of Bax showed a comparable upregulation (Fig. 2F). These results suggested that sterigmatocystin can upregulate the expression of apoptotic related genes.

3.2. Inhibition of XIAP expression contributes to sterigmatocystin induced cell death

In the differentially expressed genes upon sterigmatocystin treatment, we noticed that XIAP expression was downregulated. XIAP plays a crucial role in the inhibition of apoptotic induction, we speculated that sterigmatocystin might induce apoptosis by inhibiting XIAP expression. To identify this hypothesis, we first examined whether the expression of XIAP will be changed upon sterigmatocystin treatment. The results illustrated in Fig. 3A showed that the mRNA level of xiap was indeed dramatically downregulated upon sterigmatocystin treatment with a concentration of 60 $\mu\text{g/ml}$ while Caspase 3 showed an upregulation (Fig. 3B). Consistent with the above, western blot analysis also showed a remarkable decrease of XIAP expression and a resultant increase of cleaved caspase 3 and PARP expression in sterigmatocystin treated cells (Fig. 3C&D). We also noticed that XIAP and Caspase 3 colocalized in the cells upon sterigmatocystin treatment (Fig. 3E). To study whether overexpression of XIAP has an effect on apoptosis of liver cancer cells. we performed flow cytometry analysis. HepG2 cells were treated with overexpression of XIAP and sterigmatocystin (60 $\mu\text{g/ml}$) alone and in combination. The results demonstrated that XIAP overexpression inhibited liver cancer cells apoptosis. However, sterigmatocystin treatment alone and sterigmatocystin combined with XIAP treatment promoted the apoptosis of hepatoma cells (Fig. 3F&G).

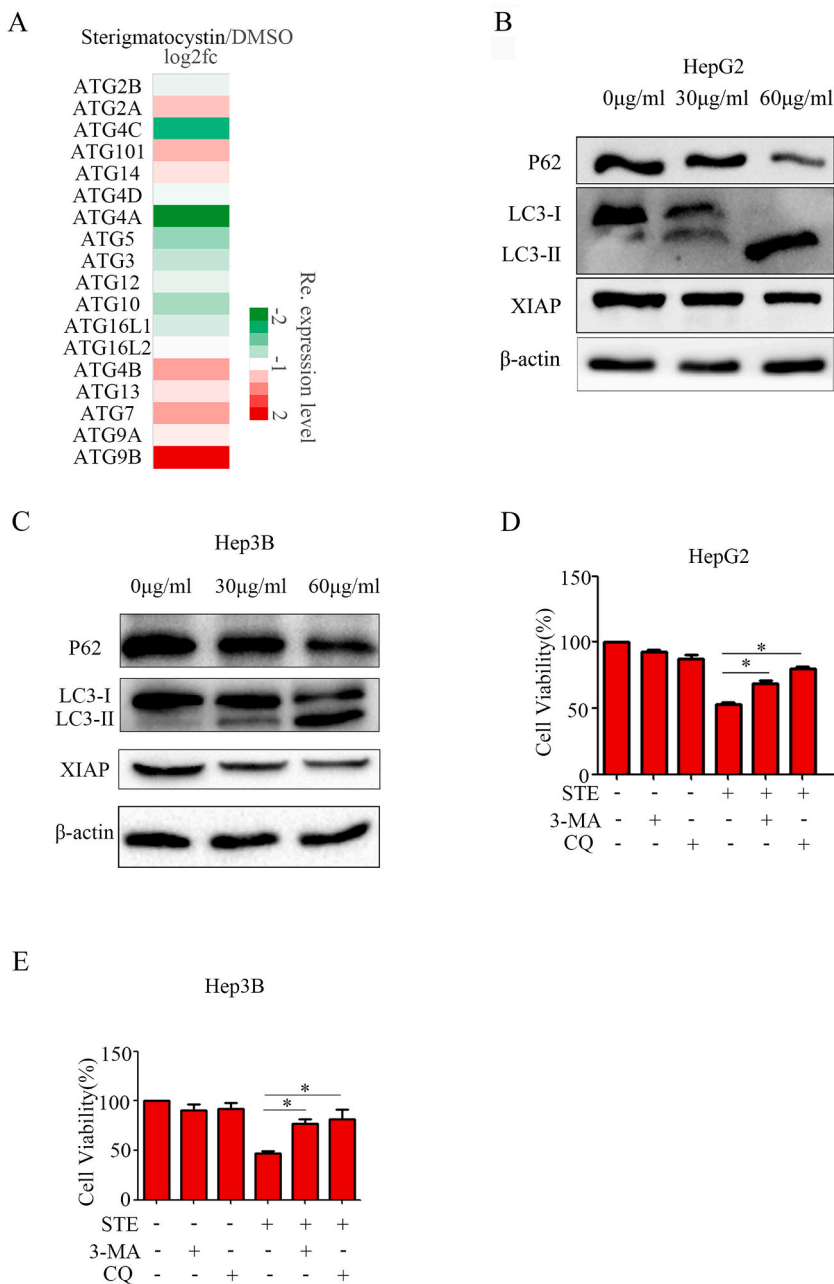
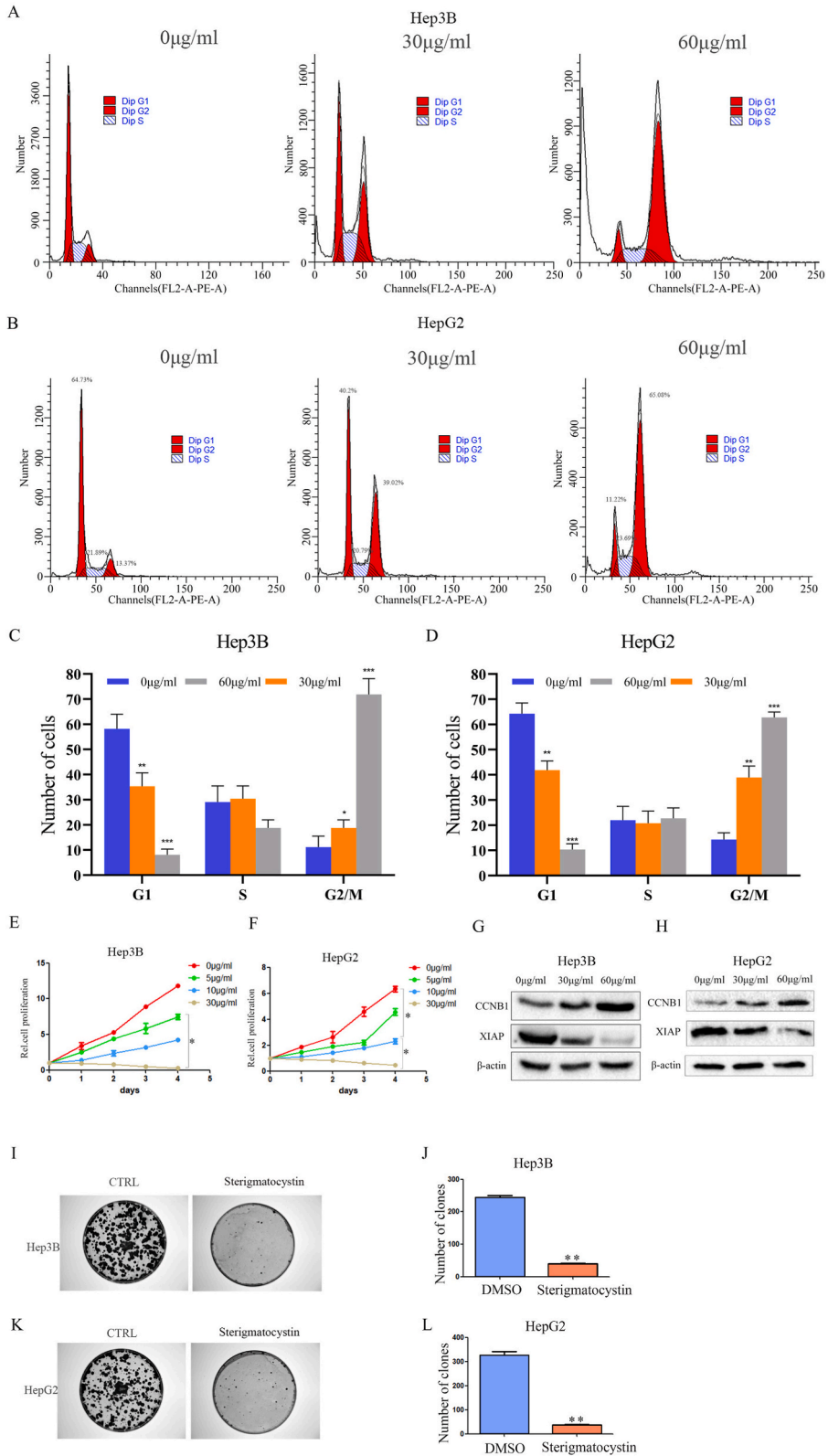


Fig. 4. Sterigmatocystin treatment induces the expression of autophagy related genes. (A) The relative expression of autophagy related genes in transcriptome analysis was shown. (B&C) The protein expression levels of p62 and LC3 were detected by western blot in HepG2 (B) or Hep3B (C) cells after treatment with sterigmatocystin at concentrations of 0 µg/ml, 30 µg/ml, and 60 µg/ml for 24 h. β-actin was used as loading control. (D&E) Cell counting kit 8 (CCK8) assay was performed in HepG2 (D) or Hep3B (E) cells treated with sterigmatocystin, 3-MA or CQ alone or together as indicated. Error bars represent data from three independent experiments (mean ± SD). *P < 0.05.



(caption on next page)

Fig. 5. The effects of sterigmatocystin on cell cycle progression, cell proliferation and colony formation were examined. (A–D) Flow cytometric analysis of cell cycle in Hep3B (A&C) or HepG2 (B&D) cells after treatment with sterigmatocystin at concentrations of 0 $\mu\text{g/ml}$, 30 $\mu\text{g/ml}$, and 60 $\mu\text{g/ml}$ for 24 h (E&F) Cell counting kit 8 (CCK8) assay was performed in Hep3B (E) or HepG2 (F) cells after treatment with sterigmatocystin at concentrations of 0 $\mu\text{g/ml}$, 30 $\mu\text{g/ml}$, and 60 $\mu\text{g/ml}$ for 24 h. Error bars represent data from three independent experiments (mean \pm SD). * $P < 0.05$. (G&H) The protein expression levels of cyclin B1 were detected by western blot in Hep3B (G) or HepG2 (H) cells after treatment with sterigmatocystin at concentrations of 0 $\mu\text{g/ml}$, 30 $\mu\text{g/ml}$, and 60 $\mu\text{g/ml}$ for 24 h. β -actin was used as loading control. (I–L) Colony formation assay was performed to detect the effect of sterigmatocystin on Hep3B (I&J) and HepG2 (K&L) cells. Error bars represent data from three independent experiments (mean \pm SD). * $P < 0.05$.

3.3. Inhibition of XIAP by sterigmatocystin upregulates autophagy

Besides its role in apoptotic inhibition, XIAP is additionally involved in autophagy regulation by acting as a negative moderator in liver cancer cells [32,33,39,40]. To explore the detailed mechanism underlying the apoptotic induction by XIAP, we first examined whether sterigmatocystin treatment of liver cancer cells can lead to the expression of autophagy-related genes. Analysis of the transcriptome data revealed a noticeable increase in the expression levels of a group of genes related to autophagy following sterigmatocystin treatment (Fig. 4A). Interestingly, sterigmatocystin treatment resulted in the LC3I conversion to LC3II, while p62 presented a decreasing expression pattern (Fig. 4B&C).

Next, we analyzed the roles of autophagy in cell death induced by sterigmatocystin. Thus, pharmacological inhibition of autophagy was applied to further investigate the relationship between autophagy and apoptosis induction following sterigmatocystin treatment. As shown in Fig. 4D, combined treatment of sterigmatocystin with autophagy inhibitor (CQ or 3-methyladenine, 3-MA) led to a relief of cytotoxicity in HepG2 cells, and similar outcomes were observed in Hep3B cells (Fig. 4E), indicating that the activation of autophagy induced by sterigmatocystin contributes to cytotoxicity.

Sterigmatocystin treatment induces cell cycle arrest, blocks cell proliferation, and slows down colony formation in liver cancer cells.

To investigate the changes in the cell cycle of liver cancer cells after sterigmatocystin treatment, we performed flow cytometry analysis. Hep3B and HepG2 cells were treated with varying concentrations of sterigmatocystin for 24 h, followed by PI staining and flow cytometry analysis. The results showed that the G1/S phase of the cells treated with sterigmatocystin was shortened, while the G2/M phase became longer (Fig. 5A–D).

Since sterigmatocystin can cause cell apoptosis and change the cell cycle pattern in liver cancer cells, we further investigated whether it has an effect on cell proliferation. To answer this question, a cell proliferation experiment was performed. Cell proliferation was detected by measuring cell survival at a period of four days. It was found that the growth of Hep3B and HepG2 cells treated with higher concentration of sterigmatocystin was significantly inhibited, indicating that the proliferation of liver cancer cells was dose-dependently suppressed by sterigmatocystin treatment (Fig. 5E&F). In agreement with the findings mentioned earlier, western blot analysis demonstrated that CCNB1 expression peaked under high concentration of sterigmatocystin treatment (Fig. 5G&H). Moreover, the colony formation assay demonstrated a decrease in the number of clones formed by Hep3B and HepG2 cells following sterigmatocystin treatment, indicating the ability of the cells to form clones was inhibited (Fig. 5I–L). Together, these data implied that sterigmatocystin can induce cell cycle arrest, prevents cell proliferation, and slow down colony formation in liver cancer cells.

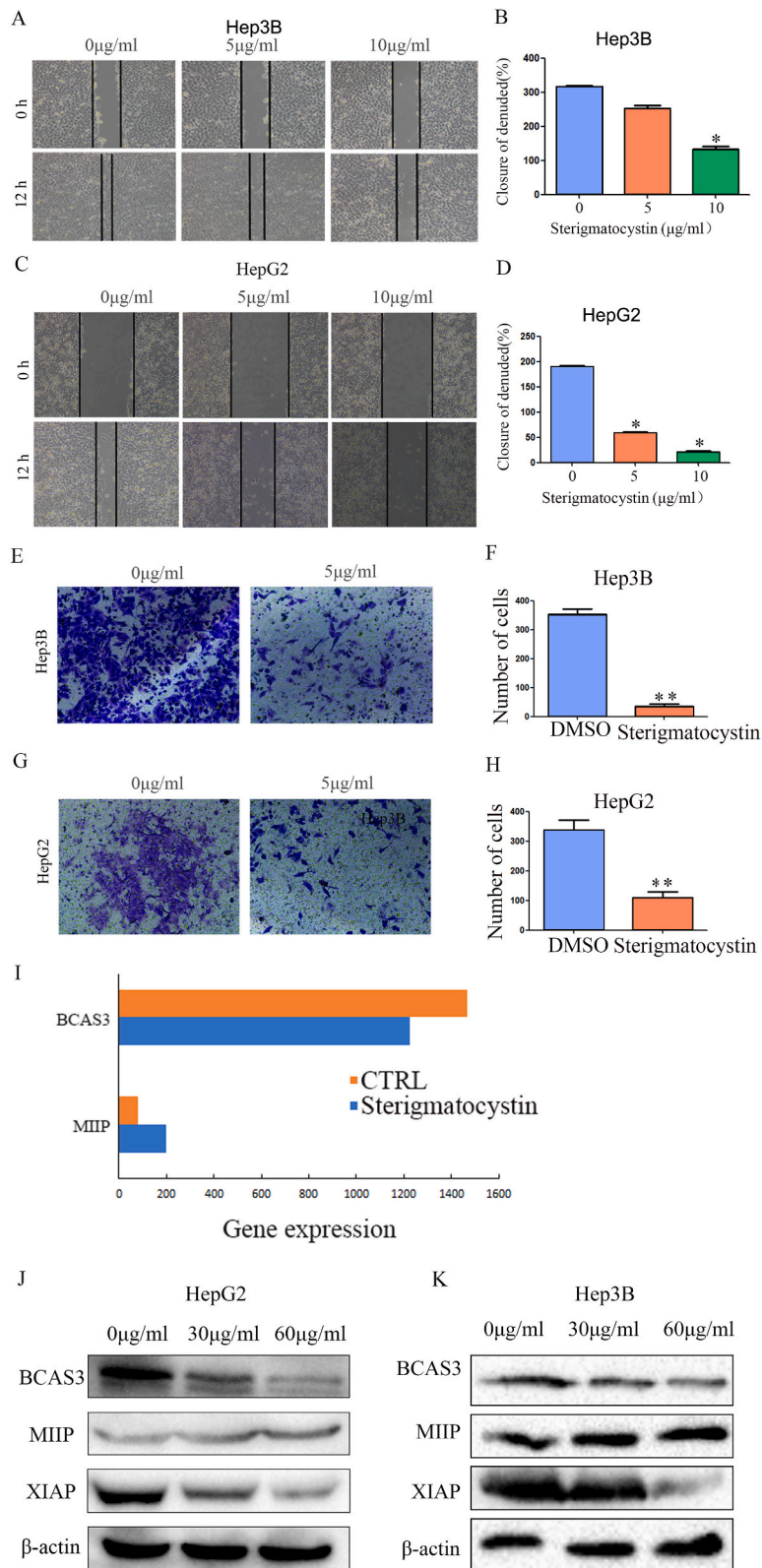
3.4. Sterigmatocystin inhibits the migration and invasion of liver cancer cells

The roles of XIAP in driving the metastasis of hepatocellular carcinoma and bladder cancers has been elucidated [41–43]. To investigate whether sterigmatocystin has an impact on liver cancer cell migration and invasion, we treated Hep3B and HepG2 cells with different concentrations of sterigmatocystin to assess the migration and invasion capabilities of the liver cancer cells. As shown in Fig. 6A–D, the wound healing assay demonstrated that sterigmatocystin treatment could effectively inhibit cell migration. Notably, the migration capacity of liver cancer cells decreased significantly following sterigmatocystin treatment compared to the control group. In addition, the transwell invasion assay showed a remarkable decrease in the invasion ability of Hep3B and HepG2 cells following treatment with various concentrations of sterigmatocystin, resulting in a reduced number of cells entering the chamber. (Fig. 6E–H). In line with the above results, transcriptome assay and western blot analysis revealed that the metastasis-related protein MIIP (migration and invasion inhibitory protein) was downregulated while BCAS3 (Breast carcinoma amplified sequence 3) was upregulated (Fig. 6I–K).

3.5. Sterigmatocystin exhibits a therapeutic effect on tumor growth

To assess whether sterigmatocystin exhibits anti-tumor effects against hepatoma cells, as shown in Fig. 7A&B, sterigmatocystin treatment led to a decrease in cell viability in a dose-dependent manner. Based on the inhibitory ratio, the half-maximal inhibitory concentration (IC50) values of sterigmatocystin in Hep3B and HepG2 cells were approximately 35 and 60 $\mu\text{g/ml}$, respectively.

In order to assess the safety of using sterigmatocystin in mice, we dissolved DMSO and sterigmatocystin in distilled water and administered it to mice orally for a duration of seven days. We observed that there was no pathological effect on the liver of normal



(caption on next page)

Fig. 6. Sterigmatocystin treatment inhibits cell migration and invasion of liver cancer cells. (A–D) Wound-healing assay was performed to measure the migration of hepatoma cells with sterigmatocystin treatment as indicated concentration and time. The wound edges are marked by black lines (A and C). The wound closure percentage is shown (B and D). The results represent the mean \pm SEM of triplicate experiments. * $P < 0.05$. (E–H) The effect of sterigmatocystin on cell invasion was measured in Hep3B (E) or HepG2 (G) cells by Matrigel transwell assays. The quantitative results are shown in (F) and (H) respectively. The results represent the standard deviation (SD) of triplicate experiments. * $P < 0.05$; ** $P < 0.01$. (I) The expression of MIIP and BCAS3 in transcriptome analysis was shown. (J&K) The protein expression levels of BCAS3 and MIIP were detected by western blot in HepG2 (J) or Hep3B (K) cells after treatment with sterigmatocystin at concentrations of 0 $\mu\text{g/ml}$, 30 $\mu\text{g/ml}$, and 60 $\mu\text{g/ml}$ for 24 h. β -actin was used as loading control.

nude mice after treatment with sterigmatocystin (Fig. 7C). To evaluate the potential anti-tumor properties of sterigmatocystin *in vivo*, nude mice with subcutaneous tumors were injected with DMSO and sterigmatocystin. The results illustrated in Fig. 7D displayed a significant suppression of tumor growth in HepG2 xenograft nude mice following sterigmatocystin treatment compared to the control group, as evident from changes in tumor size (Fig. 7E), tumor volume (Fig. 7F), and tumor weight (Fig. 7G). Taken together, these observations suggested that inhibition of XIAP by sterigmatocystin might contribute to the induction of apoptotic and autophagic cell death in liver cancer cells (Fig. 7H).

4. Discussion

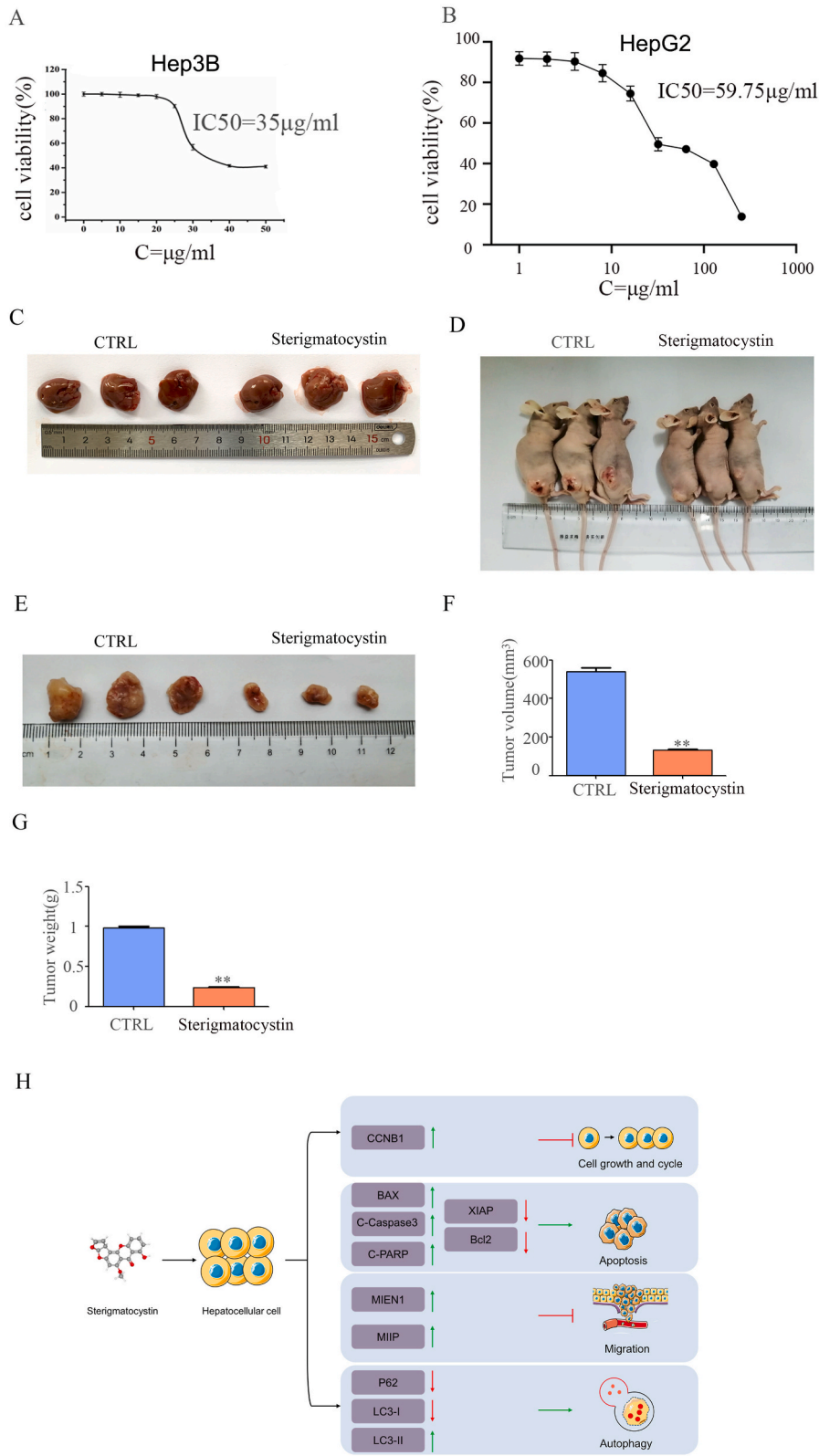
Liver cancer ranks the top five most common malignant tumors with poor prognosis [1]. Due to lack of early detection methods, most of the patients diagnosed with liver cancer have entered the advanced stage of tumors. In addition, due to lack of effective drugs, the poor effect of surgical treatment, combined with the recurrence, metastasis, and postoperative infection, the patients often have low five-year survival rate after receiving formal professional treatment. After the surgical operation, chemotherapy is usually used to prolong the survival period of the patients. But traditional chemical treatment has low clinical effect and often leads to obvious serious side effects. Moreover, many patients use these drugs for a long time, which is very easy to produce drug resistance and affects the therapeutic effect. Therefore, it is crucial to explore the mechanisms of liver cancer and develop new anti-cancer drugs that are both more efficient and have fewer side effects.

With the continuous search for anti-cancer drugs, more than 170 small molecular compounds have been found in human beings, and more than 130 are natural. More than 60 compounds are fungal extracts, which play a crucial role in inhibiting cell proliferation and enhancing apoptosis, and they possess a remarkably stable chemical structure and exhibit unique molecular activity. Sterigmatocystin, a fungal metabolite, has been identified as capable of inducing cytochrome C release and promoting apoptosis in U2OS and MG63 osteosarcoma cell lines [36]. The potential of sterigmatocystin to suppress liver cancer cells proliferation, induce apoptosis, and uncover the underlying mechanism remains to be explored. Our research found that it can inhibit liver cancer cells proliferation and migration, as well as inhibition of tumor growth. However, because the sample size used in animal experiments is small, it is necessary to enlarge the sample content in the follow-up study to detect the therapeutic effects of sterigmatocystin. In addition, the safety of the drug needs to be evaluated. Finally, the increased expression of anti-apoptotic proteins in cancer treatment can lead to increased resistance. Therefore, it is expected that by specifically targeting and inhibiting these proteins, the effectiveness of chemotherapy will be improved [44]. Our study demonstrated that sterigmatocystin can downregulate XIAP expression, whether it can lower drug resistance, and whether it can be combined with chemotherapy drugs to improve the effect of chemotherapy are worth further research.

Apoptosis is a strictly regulated process of programmed cell death, which is directly or indirectly related to the occurrence of various diseases. For example, autoimmune diseases, and so on, many factors that can induce apoptosis, such as radiation, drugs, etc. Caspases are recognized to have a crucial function in the process of apoptosis. They are categorized into initiator and effector caspases, which play important roles in the upstream and downstream of death signal transduction respectively. XIAP is known to interact with and degrade both initiator and effector caspases, thereby contributing to the inhibition of apoptosis. Through transcriptome analysis, we found that sterigmatocystin can lower the transcription level of XIAP, thus improving the level of cleaved caspase and promoting apoptosis. However, there are limitations in this study that should be acknowledged. At first, the efficacy and safety of new drugs should be extensively examined. Second, it is important to investigate whether sterigmatocystin has an effect on chemoresistance and whether it can improve the effectiveness of other chemotherapy drugs in combination usage. Moreover, it is crucial to emphasize that this research does not include any clinical experimental data. Also, a mouse model of peritoneal implantation of liver cancer should be further conducted to detect invasion and metastasis, thus providing a solid scientific basis for clinical treatment. Lastly, XIAP has been shown to be involved in autophagy regulation and its role in autophagy depends on cell type and cellular content, therefore, additional investigations are warranted to explore the roles of sterigmatocystin in autophagy regulation in other types of cancer cells.

Ethics statement

All animal experiments in this study were reviewed and approved by the Institutional Animal Care and Use Committee at Chongqing University (Protocol No: 2020L0018).



(caption on next page)

Fig. 7. Sterigmatocystin treatment inhibits tumor growth. (A&B) Cell counting kit 8 (CCK8) assay was performed in Hep3B (A) and (B) HepG2 cells upon sterigmatocystin treatment. (C) Safety assessment of sterigmatocystin in mice. (D–G) Representative photos showing euthanized mice (D) and xenograft tumors (E) at 4 weeks post subcutaneous injection ($n = 3$ per group). Tumor sizes were measured every 5 days. Tumor weight (F) and tumor volume (G) were shown. Results presented represent the means of triplicate experiments \pm SEM. * $P < 0.05$; ** $P < 0.01$. (H) Schematic model showing the effects of sterigmatocystin on the cell cycle progression, cell migration and apoptosis.

Funding

This work was supported by the National Natural Science Foundation of China (Grant No. 82172888), the Fundamental Research Funds for the Central Universities (Grant No. 2023CDJYGRH-YB07 and 2023CDJXY-009) and Natural Science Foundation Project of CQ CSTC (Grant cstc2020jcyj-msxmX0154).

Data availability statement

All data used during this study are included in the submitted article.

CRediT authorship contribution statement

Xu Chen: Writing – original draft, Investigation, Data curation, Conceptualization. **Zhengping Che:** Investigation, Formal analysis, Data curation, Conceptualization. **Jiajia Wu:** Validation, Investigation, Data curation. **Cheng Zeng:** Investigation. **Xiao-long Yang:** Writing – review & editing, Resources, Methodology, Conceptualization. **Lin Zhang:** Writing – review & editing, Resources, Methodology, Data curation. **Zhenghong Lin:** Writing – review & editing, Writing – original draft, Supervision, Resources, Project administration, Methodology, Funding acquisition, Formal analysis, Data curation, Conceptualization.

Declaration of competing interest

The authors declare that they have no known competing financial interests or personal relationships that could have appeared to influence the work reported in this paper.

Acknowledgments

We thank the Analytical and Testing Center of Chongqing University for providing confocal fluorescence microscopy assistance.

Appendix A. Supplementary data

Supplementary data to this article can be found online at <https://doi.org/10.1016/j.heliyon.2024.e29567>.

References

- [1] F. Bray, J. Ferlay, I. Soerjomataram, R.L. Siegel, L.A. Torre, A. Jemal, Global cancer statistics 2018: GLOBOCAN estimates of incidence and mortality worldwide for 36 cancers in 185 countries, *CA A Cancer J. Clin.* 68 (6) (2018) 394–424.
- [2] L. Dong, L. Yu, H. Li, L. Shi, Z. Luo, H. Zhao, Z. Liu, G. Yin, X. Yan, Z. Lin, An NAD(+)-Dependent deacetylase SIRT7 promotes HCC development through deacetylation of USP39, *iScience* 23 (8) (2020) 101351.
- [3] L. Wang, W. Su, Z. Liu, M. Zhou, S. Chen, Y. Chen, D. Lu, Y. Liu, Y. Fan, Y. Zheng, et al., CD44 antibody-targeted liposomal nanoparticles for molecular imaging and therapy of hepatocellular carcinoma, *Biomaterials* 33 (20) (2012) 5107–5114.
- [4] J.F. Kerr, A.H. Wyllie, A.R. Currie, Apoptosis: a basic biological phenomenon with wide-ranging implications in tissue kinetics, *Br. J. Cancer* 26 (4) (1972) 239–257.
- [5] T.M. Buttke, P.A. Sandstrom, Oxidative stress as a mediator of apoptosis, *Immunol. today* 15 (1) (1994) 7–10.
- [6] S. McComb, P.K. Chan, A. Guinot, H. Hartmannsdottir, S. Jenni, M.P. Dobay, J.P. Bourquin, B.C. Bornhauser, Efficient apoptosis requires feedback amplification of upstream apoptotic signals by effector caspase-3 or -7, *Sci. Adv.* 5 (7) (2019) eaau9433.
- [7] S.W. Tait, D.R. Green, Mitochondria and cell death: outer membrane permeabilization and beyond, *Nat. Rev. Mol. Cell Biol.* 11 (9) (2010) 621–632.
- [8] S.W. Tait, D.R. Green, Mitochondria and cell signalling, *J. Cell Sci.* 125 (Pt 4) (2012) 807–815.
- [9] M. Donepudi, M.G. Grutter, Structure and zymogen activation of caspases, *Biophys. Chem.* 101–102 (2002) 145–153.
- [10] N.A. Thornberry, Y. Lazebnik, Caspases: enemies within, *Science* 281 (5381) (1998) 1312–1316.
- [11] B.P. Eckelman, G.S. Salvesen, The human anti-apoptotic proteins cIAP1 and cIAP2 bind but do not inhibit caspases, *J. Biol. Chem.* 281 (6) (2006) 3254–3260.
- [12] G.S. Salvesen, C.S. Duckett, IAP proteins: blocking the road to death's door, *Nat. Rev. Mol. Cell Biol.* 3 (6) (2002) 401–410.
- [13] A.D. Schimmer, Inhibitor of apoptosis proteins: translating basic knowledge into clinical practice, *Cancer Res.* 64 (20) (2004) 7183–7190.
- [14] Q.L. Deveraux, J.C. Reed, IAP family proteins—suppressors of apoptosis, *Gene Dev.* 13 (3) (1999) 239–252.
- [15] Q.L. Deveraux, E. Leo, H.R. Stennicke, K. Welsh, G.S. Salvesen, J.C. Reed, Cleavage of human inhibitor of apoptosis protein XIAP results in fragments with distinct specificities for caspases, *EMBO J.* 18 (19) (1999) 5242–5251.
- [16] Y. Suzuki, Y. Nakabayashi, K. Nakata, J.C. Reed, R. Takahashi, X-linked inhibitor of apoptosis protein (XIAP) inhibits caspase-3 and -7 in distinct modes, *J. Biol. Chem.* 276 (29) (2001) 27058–27063.
- [17] M. Gyrd-Hansen, M. Darding, M. Miasari, M.M. Santoro, L. Zender, W. Xue, T. Tenev, P.C. da Fonseca, M. Zvelebil, J.M. Bujnicki, et al., IAPs contain an evolutionarily conserved ubiquitin-binding domain that regulates NF-kappaB as well as cell survival and oncogenesis, *Nat. Cell Biol.* 10 (11) (2008) 1309–1317.

- [18] A.J. Schile, M. Garcia-Fernandez, H. Steller, Regulation of apoptosis by XIAP ubiquitin-ligase activity, *Gene Dev.* 22 (16) (2008) 2256–2266.
- [19] K. Rajalingam, I. Dikic, Inhibitors of apoptosis catch ubiquitin, *Biochem. J.* 417 (1) (2009) e1–e3.
- [20] D. Vucic, H.R. Stennicke, M.T. Pisabarro, G.S. Salvesen, V.M. Dixit, ML-IAP, a novel inhibitor of apoptosis that is preferentially expressed in human melanomas, *Curr. Biol. : CB* 10 (21) (2000) 1359–1366.
- [21] H. Harlin, S.B. Reffey, C.S. Duckett, T. Lindsten, C.B. Thompson, Characterization of XIAP-deficient mice, *Mol. Cell Biol.* 21 (10) (2001) 3604–3608.
- [22] Y. Fuchs, S. Brown, T. Gorenc, J. Rodriguez, E. Fuchs, H. Steller, Sept 4/ARTS regulates stem cell apoptosis and skin regeneration, *Science* 341 (6143) (2013) 286–289.
- [23] E. Koren, Y. Yosefzon, R. Ankawa, D. Soteriou, A. Jacob, A. Nevelsky, R. Ben-Yosef, G. Bar-Sela, Y. Fuchs, ARTS mediates apoptosis and regeneration of the intestinal stem cell niche, *Nat. Commun.* 9 (1) (2018) 4582.
- [24] M. Yabal, N. Muller, H. Adler, N. Knies, C.J. Gross, R.B. Damgaard, H. Kanegane, M. Ringelhan, T. Kaufmann, M. Heikenwalder, et al., XIAP restricts TNF- and RIP3-dependent cell death and inflammasome activation, *Cell Rep.* 7 (6) (2014) 1796–1808.
- [25] L. Dubrez, J. Berthelet, V. Glorian, IAP proteins as targets for drug development in oncology, *OncoTargets Ther.* 9 (2013) 1285–1304.
- [26] M. Krajewska, S. Krajewski, S. Banares, X. Huang, B. Turner, L. Bubendorf, O.P. Kallioniemi, A. Shabaik, A. Vitiello, D. Peehl, et al., Elevated expression of inhibitor of apoptosis proteins in prostate cancer, *Clin. Cancer Res. : an official journal of the American Association for Cancer Research* 9 (13) (2003) 4914–4925.
- [27] I. Tamm, S.M. Kornblau, H. Segall, S. Krajewski, K. Welsh, S. Kitada, D.A. Scudiero, G. Tudor, Y.H. Qui, A. Monks, et al., Expression and prognostic significance of IAP-family genes in human cancers and myeloid leukemias, *Clin. Cancer Res. : an official journal of the American Association for Cancer Research* 6 (5) (2000) 1796–1803.
- [28] R. Abbas, S. Larisch, Targeting XIAP for promoting cancer cell death—the story of ARTS and SMAC, *Cells* 9 (3) (2020).
- [29] R. Hegde, S.M. Srinivasula, Z. Zhang, R. Wassell, R. Mukattash, L. Cilenti, G. DuBois, Y. Lazebnik, A.S. Zervos, T. Fernandes-Alnemri, et al., Identification of Omi/HtrA2 as a mitochondrial apoptotic serine protease that disrupts inhibitor of apoptosis protein-caspase interaction, *J. Biol. Chem.* 277 (1) (2002) 432–438.
- [30] R. Elhasid, D. Sahar, A. Merling, Y. Zivony, A. Rotem, M. Ben-Arush, S. Izraeli, D. Bercovich, S. Larisch, Mitochondrial pro-apoptotic ARTS protein is lost in the majority of acute lymphoblastic leukemia patients, *Oncogene* 23 (32) (2004) 5468–5475.
- [31] J.P. Wing, L.M. Schwartz, J.R. Nambu, The RHG motifs of *Drosophila* Reaper and Grim are important for their distinct cell death-inducing abilities, *Mech. Dev.* 102 (1–2) (2001) 193–203.
- [32] X. Huang, Z. Wu, Y. Mei, M. Wu, XIAP inhibits autophagy via XIAP-Mdm2-p53 signalling, *EMBO J.* 32 (16) (2013) 2204–2216.
- [33] W.Y. Wu, H. Kim, C.L. Zhang, X.L. Meng, Z.S. Wu, Clinical significance of autophagic protein LC3 levels and its correlation with XIAP expression in hepatocellular carcinoma, *Med. Oncol.* 31 (8) (2014) 108.
- [34] P. Anelli, S.W. Peterson, M. Haidukowski, A.F. Logrieco, A. Moretti, F. Epifani, A. Susca, *Penicillium graminicasei*, a new species isolated from cave cheese in Apulia, Italy, *Int. J. Food Microbiol.* 282 (2018) 66–70.
- [35] S.H. Son, Y.E. Son, H.J. Cho, W. Chen, M.K. Lee, L.H. Kim, D.M. Han, H.S. Park, Homeobox proteins are essential for fungal differentiation and secondary metabolism in *Aspergillus nidulans*, *Sci. Rep.* 10 (1) (2020) 6094.
- [36] I. Caceres, A.A. Khoury, R.E. Khoury, S. Lorber, I.P. Oswald, A.E. Khoury, A. Atoui, O. Puel, J.D. Bailly, Aflatoxin biosynthesis and genetic regulation: a review, *Toxins* 12 (3) (2020).
- [37] J. Shi, G. Li, Y. Cui, Y. Zhang, D. Liu, Y. Shi, H. He, Surface-imprinted beta-cyclodextrin-functionalized carbon nitride nanosheets for fluorometric determination of sterigmatomycin, *Mikrochim. Acta* 186 (12) (2019) 808.
- [38] L. Yu, L. Dong, H. Li, Z. Liu, Z. Luo, G. Duan, X. Dai, Z. Lin, Ubiquitination-mediated degradation of SIRT1 by SMURF2 suppresses CRC cell proliferation and tumorigenesis, *Oncogene* 39 (22) (2020) 4450–4464.
- [39] C.H.A. Cheung, Y.C. Chang, T.Y. Lin, S.M. Cheng, E. Leung, Anti-apoptotic proteins in the autophagic world: an update on functions of XIAP, Survivin, and BRUCE, *J. Biomed. Sci.* 27 (1) (2020) 31.
- [40] H. Tu, M. Costa, XIAP's profile in human cancer, *Biomolecules* 10 (11) (2020).
- [41] Y.H. Shi, W.X. Ding, J. Zhou, J.Y. He, Y. Xu, A.A. Gambotto, H. Rabinowich, J. Fan, X.M. Yin, Expression of X-linked inhibitor-of-apoptosis protein in hepatocellular carcinoma promotes metastasis and tumor recurrence, *Hepatology* 48 (2) (2008) 497–507.
- [42] H. Jin, L. Xue, L. Mo, D. Zhang, X. Guo, J. Xu, J. Li, M. Peng, X. Zhao, M. Zhong, et al., Downregulation of miR-200c stabilizes XIAP mRNA and contributes to invasion and lung metastasis of bladder cancer, *Cell Adhes. Migrat.* 13 (1) (2019) 236–248.
- [43] Y. Yu, H. Jin, J. Xu, J. Gu, X. Li, Q. Xie, H. Huang, J. Li, Z. Tian, G. Jiang, et al., XIAP overexpression promotes bladder cancer invasion in vitro and lung metastasis in vivo via enhancing nucleolin-mediated Rho-GD β mRNA stability, *Int. J. Cancer* 142 (10) (2018) 2040–2055.
- [44] N. Shahar, S. Larisch, Inhibiting the inhibitors: targeting anti-apoptotic proteins in cancer and therapy resistance, *Drug Resist. Updates : reviews and commentaries in antimicrobial and anticancer chemotherapy* 52 (2020) 100712.